

Heterojunction ZnO on Silicon for Potential UV to Visible Photodetector Utilising SILVACO TCAD Effect of Thickness and Doping

A. Azmi¹, A. F. Abd Rahim^{1,*}, N. S. Mohd Razali¹, R. Radzali¹, A. Mahmood², I. H Hamzah¹, M. H. Abdullah¹
and M. F. Packer Mohamed³

¹Centre for Electrical Engineering Studies, Universiti Teknologi MARA, Cawangan Pulau Pinang, Permatang
Pauh Campus, 13500 Pulau Pinang, MALAYSIA

²Department of Applied Sciences, Universiti Teknologi MARA, Cawangan Pulau Pinang, 13500 Permatang
Pauh, Pulau Pinang, Malaysia

³School of Electrical and Electronic Engineering, Engineering Campus, Universiti Sains Malaysia, 14300
Nibong Tebal, Penang, Malaysia

*corresponding author: alhan570@uitm.edu.my

ARTICLE HISTORY

ABSTRACT

Received
30 June 2022

Accepted
6 August 2022

Available online
20 September 2022

In this work, the study of heterojunction Zinc Oxide on Silicon to enhance UV photodetector performance has been conducted. The study was carried out using a SILVACO ATLAS device simulator. There are two parameters studied in this project are: to find the best thickness of ZnO and suitable doping concentration of ZnO on the silicon substrate as a photodetector device. There are three different thicknesses of ZnO (0.5 μm , 1 μm and 2 μm) and four different doping concentrations of ZnO applied ($1 \times 10^{15} \text{ cm}^{-3}$, $1 \times 10^{19} \text{ cm}^{-3}$, $1 \times 10^{20} \text{ cm}^{-3}$ and $1 \times 10^{21} \text{ cm}^{-3}$). The performance of the ZnO on Si as a photodetector was evaluated by dark and photo current-voltage (I-V) characteristics. It was found that the optimum thickness of ZnO is at 1 μm and the suitable doping concentration of ZnO is at $1 \times 10^{21} \text{ cm}^{-3}$ since with these values, the photocurrent response is high, and in spectral response, the peak value for both is depicted in a visible region, which is suitable as UV photodetector device criteria.

Keywords: ZnO, UV photodetector, Schottky Barrier Height, Spectral Response, SILVACO

1. INTRODUCTION

Ultraviolet(UV) photodetectors are important due to their many industrial applications, such as processing semiconductor devices, detecting missiles, space communication, nuclear reactor monitoring and ozone monitoring[1]. This project focuses on the importance of the UV photodetector in semiconductor devices, where the photons are captured in the semiconductor detectors in the bulk of the semiconductor material, creating electron-hole pairs that are separated by an electric field. Such detectors use the internal photoelectric effect where the photons' energy is sufficiently high to excite the electrons into the semiconductor material's conduction band. In the case of photovoltaic detectors, the electron-hole pairs are isolated by the electrical field of p-n junctions, the Schottky barrier, or metal-insulator-semiconductor (MIS) condensers. This leads to an intrinsic photocurrent proportional to the number of photons observed. Applying a voltage across the absorbing region causes a current to flow in proportion

to the intensity of the incident radiation [2]. UV light is a general term for a specific electromagnetic radiation band with a wavelength range of 100–400 nm and a range of 3.1–12.4 eV for energy distribution. Therefore, the material used to enhance the detection of the UV ray in the semiconductor industry is also essential. ZnO is one of the suitable materials since it has high electron mobility, high thermal conductivity, broad and direct band gap and large exciton binding energy. These characteristics make ZnO suitable for a wide range of devices such as transparent thin-film transistors, photodetectors, light-emitting diodes and laser diodes operating in the spectrum's blue and ultraviolet regions [3]. However, the lack of control over its electrical conductivity has hampered the use of ZnO as a semiconductor in electronic devices, where ZnO crystals are almost always n-type [4], and they suffer from a lack of reproducibility of high-quality p-type epitaxial growth and agglomeration of ZnO nanoparticles. Therefore, the type of substrate material to be heterojunction with ZnO is critical since it also plays a vital role in determining the structural, electrical, optical, and mechanical properties and range of application of growing nanostructures in future.

Several p-type materials have been heterojunction with ZnO as the host material, such as Gallium Nitride (GaN), Nickel Oxide (NiO), Strontium Copper Oxide ($\text{Sr}_2\text{Cu}_2\text{O}_2$) and Silicon (Si) [5]. Among many p-type materials mentioned, Si is the most suitable material since it is a crucial material in the microelectronics industry. Silicon has high quality and a large area p-type substrate available at low cost when manufactured. The heterojunction photodetector of ZnO on Si (ZnO/Si) is expected to have the ability to simultaneously detect both UV and visible wavelengths over a single framework, which is very useful in many industrial applications. Other benefits of ZnO/Si heterojunction are its good optical and electrical properties, fabrication simplicity, relatively low deposition temperature and low cost of fabrication, all of which are why the researchers have drawn a significant interest in using it in the field of photodetectors [6].

In this study, the ZnO layer was deposited on top of the bulk Silicon substrate with different thicknesses and doping concentrations, and it was simulated using SILVACO Technology Computer-Aided Design (TCAD) tools. The SILVACO tool is a powerful TCAD tool capable of simulating semiconductor device fabrication and its electrical characteristics[7]. In this project, the structural, optical, and electrical characteristic of the ZnO/Si devices are analysed towards the UV light detection. The fabrication time can be reduced by using the simulation, and the optimum condition of the ZnO/Si as a UV photodetector can be obtained while the device's expected performance can be predicted.

2. METHODOLOGY

In this project, the virtual fabrication of the heterojunction ZnO on silicon is carried out to study its performance enhancing the UV photodetector by utilising SILVACO TCAD software. In this project, two tools from SILVACO TCAD, the ATLAS device simulator and TONYPLOT graphical tool, were used. Figure 1 shows the flow for carrying out the project. In the first part of the study, which is to investigate the effect of ZnO thickness, the process began by constructing the ZnO/Si structures for three different thicknesses (0.5 μm , 1 μm and 2 μm) of the ZnO layers in the ATLAS simulator. Initially, The structure was initialised by defining the region size and mesh for the silicon substrate at the bottom, followed by defining

the ZnO layer on top of it. The region set for the silicon substrate was $1\ \mu\text{m} \times 4\ \mu\text{m}$ and for ZnO $1\ \mu\text{m} \times$ (three different thicknesses). Figure 2 shows the ZnO/Si heterostructure displayed using TONYPLOT.

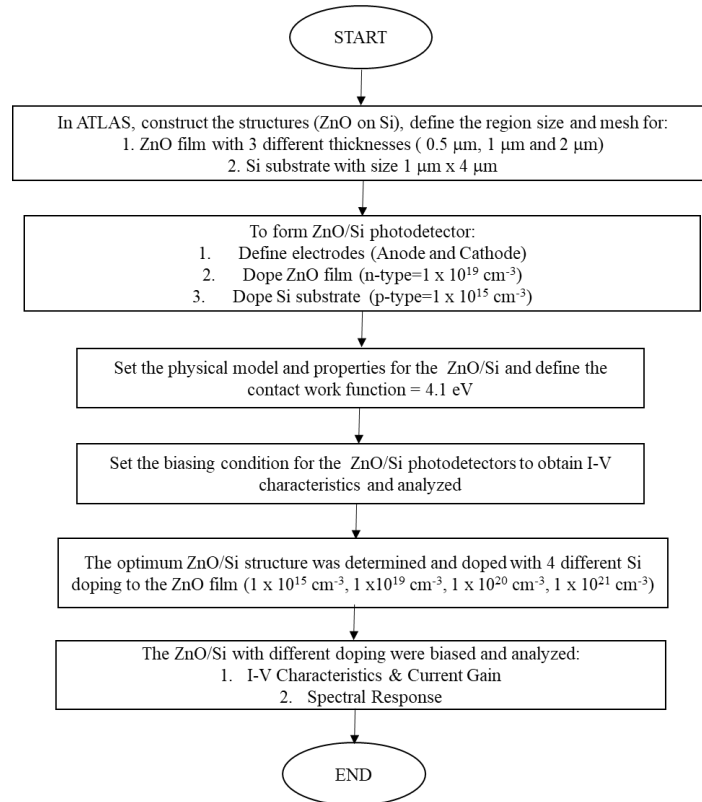


Figure 1: Flowchart for construction of ZnO/Si and characterisation of the device using ATLAS device simulator.

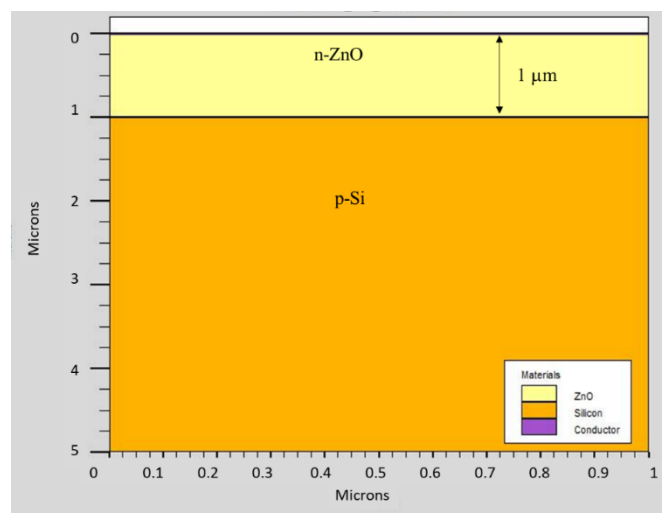


Figure 2: ZnO/Si structure with $1\ \mu\text{m}$ ZnO thickness

Next, a electrodes (anode and cathode) to form structures as a photodetector, and their positions were determined. Then, the ZnO and Si substrates were doped with a donor concentration of $1 \times 10^{19} \text{ cm}^{-3}$ and acceptor concentration of $1 \times 10^{15} \text{ cm}^{-3}$ to form n and p-type regions, respectively. The physical model parameters used for the ZnO, and Si were defined as shown in Table 1.

Table 1: Physical parameters of ZnO/Si heterostructure

| Parameters | n-ZnO | p-Si |
|--|--------|---------|
| Optical Band Gap (eV) | 3.28 | 1.12 |
| Electronic Affinity (eV) | 4.35 | 4.05 |
| Relative Permittivity ϵ_r | 8.12 | 11.8 |
| Density of states in the conduction band N_C (cm^{-3}) | 2.2e18 | 2.8e19 |
| Density of states in the valence band N_V (cm^{-3}) | 1.8e19 | 1.04e19 |
| Electron mobility μ_n ($\text{cm}^2/\text{V.s}$) | 100 | 1417 |
| Hole mobility μ_p ($\text{cm}^2/\text{V.s}$) | 25 | 470 |

The physical parameters used for the ZnO/Si heterostructure followed M. Manuoa et al. al., which adopted the Poisson equation, and electron and hole continuity equations. For carriers with drift-diffusion, the Fermi statistics were utilised. The recombination models, Shockley-Read-Hall (SRH) and Auger were incorporated into the simulation as a function of doping concentration. Thermionic emission was also included across the n-ZnO/p-Si contact [8]. As for the contact for this structure, Aluminum (Al) metal was used with 4.1 eV of work function defined. Finally, to characterise the current-voltage (I-V) characteristics and spectral response of the ZnO/Si photodetector, the solution specification, which uses the command log to solve, load and save, was defined. The device was biased under dark and photo illumination. The I-V and spectral response of the devices was plotted and analysed using TONYPLOT. The optimum thickness of ZnO was determined by the device which exhibited the highest photo response. The second part investigates the effect of doping concentration in the ZnO layer. The similar processes to construct and set the physical parameters were repeated when varying the doping concentrations ($1 \times 10^{15} \text{ cm}^{-3}$, $1 \times 10^{19} \text{ cm}^{-3}$, $1 \times 10^{20} \text{ cm}^{-3}$, $1 \times 10^{21} \text{ cm}^{-3}$) of the Zinc Oxide layer. The ZnO/Si photodetector with the different doping was then analysed.

3. RESULTS AND DISCUSSION

3.1. Structure of ZnO/Si with Different Thicknesses of ZnO

The thickness of the Si substrate was set at the constant value of $4 \mu\text{m}$, while the thickness of ZnO was varied ($0.5 \mu\text{m}$, $1 \mu\text{m}$ and $2 \mu\text{m}$). Figure 3 shows the structure of ZnO/Si with $0.5 \mu\text{m}$ thickness with mesh definition.

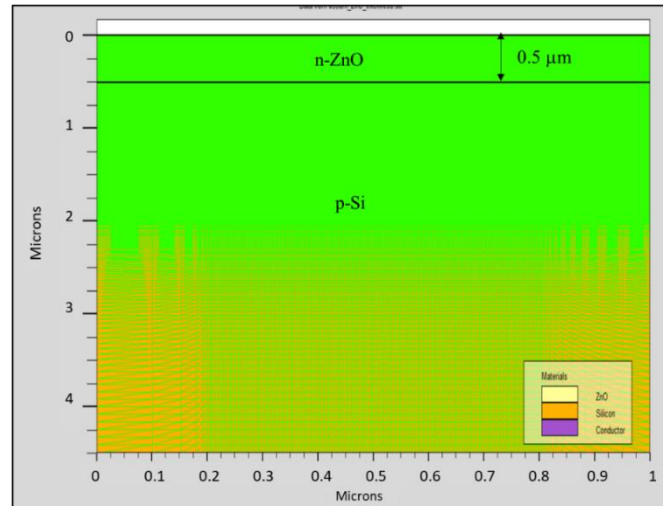


Figure 3: The structure of 0.5 μm ZnO/ Si with mesh.

3.2. I-V Characteristics of ZnO/Si with Different Thicknesses of ZnO

Figure 4 shows the I-V characteristics of the ZnO/Si photodetector measured under dark (I_d) and illumination (I_p) for the three different thicknesses of the ZnO layer. Under dark conditions, the three devices are shallow. Upon the illumination with light, the currents responded tremendously. Specifically, the highest current obtained under illumination was obtained by the 1 μm device, 8.17×10^{-6} A, followed by the 2 μm and 0.5 μm devices 6.50×10^{-6} A and 1.85×10^{-6} A respectively at 5V bias. It can be noted that the increasing ZnO thicknesses enhance the current photo response. However, it is observed that the thickness of the ZnO has its limit to exhibit the increased current upon exposure to light. The current response is observed to decrease when the thickness of Zinc Oxide is thicker than 1 μm in this work. L. Chabane et al. show that the increased thickness of Zinc Oxide films caused the degradation of the rectifying behavior, indicating significant changes in the interface's state, thus affecting the photo-response and photovoltaic response [9].

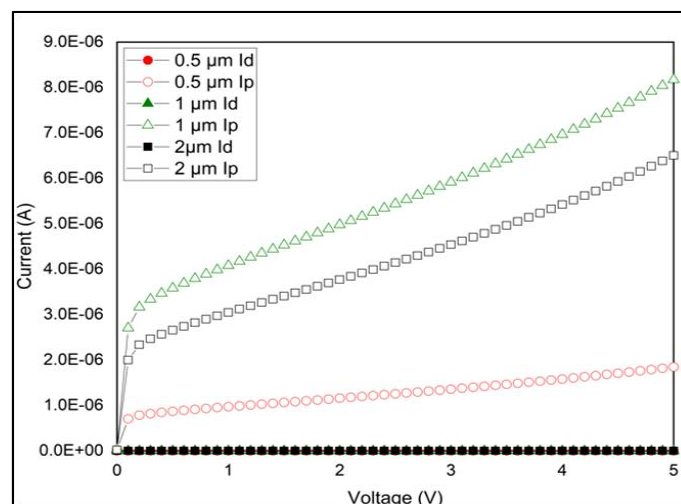


Figure 4: Current-Voltage Characteristics of ZnO/Si with Different Thickness of ZnO

The performance of the photodetector was then probed by measuring the current gain. The current gain is the ratio of the current under illumination to the current under dark. Figure 5 shows the gain for the three different thicknesses of the ZnO/Si devices. It is shown that the highest gain is obtained by the 0.5 μm device, followed by the 1 μm and 2 μm devices, respectively. This indicates that even though the 0.5 μm device does not have the highest photocurrent, its lowest dark current helps gain the highest photo response among the other devices [9].

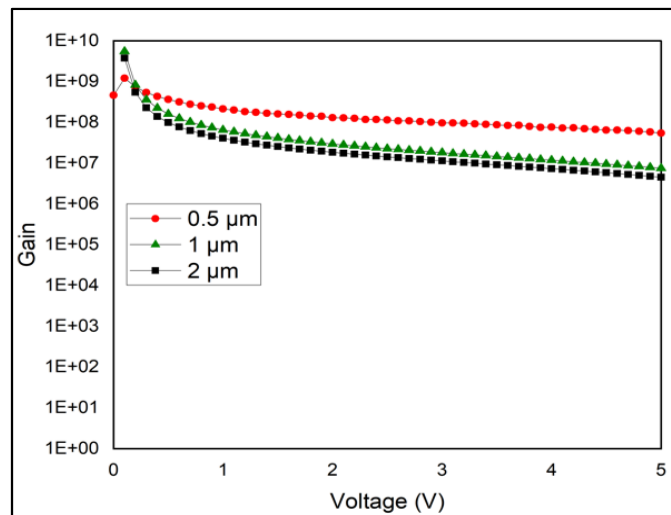


Figure 5: Gain of ZnO/Si with three different thicknesses of ZnO.

The consistency of the interface between the deposited ZnO and the semiconductor surface (the Si substrate) and the existence of the current transport through this interface defines the efficiency and reliability of the Schottky contact. Therefore, the contact's Schottky barrier height (SBH) needs to be determined [10]. The I-V characteristics of the ZnO/Si devices were analysed assuming that the thermionic emissions are the dominant current transport mechanism. According to this hypothesis, the I-V relationship of a Schottky diode is established by [11]:

$$I_d = I_o \exp\left(\frac{qV_d}{nkT}\right) \left[1 - \exp\left(\frac{-qV_d}{kT}\right)\right] \quad (1)$$

Where q is the electron charge, V_d is the applied voltage, k is the Boltzmann constant, T is the absolute temperature (approximately 300K), n is the ideality factor, and I_o is the saturation current given by the relation,

$$I_o = AA^{**}T^2 \exp\left[\frac{-q\phi_B}{kT}\right] \quad (2)$$

where A is the contact area, A^{**} is the effective Richardson constant (approximately $32 \text{ A cm}^{-2} \text{ K}^{-2}$) for ZnO, and ϕ_B is the Schottky barrier height (SBH) [12]. From equation (1), it can be simplified to

$$I_d = I_o \exp\left(\frac{qV_d}{kT}\right) \quad (3)$$

The theoretical value of A^{**} can be calculated using $A^{**} = 4\pi m^* q k^2 / h^3$. A straight line with a slope of $q/(nkT)$ will be given by the plot of $\ln I_d$ vs V_d , and the intercept with y-axis will produce I_o , in which Schottky barrier height, ϕ_B can be obtained using Equation (2) and the n , Ideality factor can be extracted from the slope. Table 2 shows the extracted parameters from the I-V characteristics: the SBH, ideality factor and series resistance determined from Equations (1) to (3) above. It can be observed that the increasing ZnO thickness increases the SBH value. Meanwhile, the ideality factor and the resistance decrease as the ZnO thickness increases. Specifically, the 0.5 μm thickness had the highest ideality factor of 8.0612 and the lowest value of SBH = 0.6303 eV. The 0.5 μm device obtained the lowest dark current (3.93×10^{-14} A) compared to the 1 μm (1.08×10^{-12} A) and 2 μm (1.43×10^{-12} A) devices which in turn resulted in the high resistance. The high ideality factor and low barrier height values of the 0.5 μm device obtained can be related to interfacial defects, various current transport processes, inhomogeneities in the interface oxide layer, and the diode's series resistance [13]. Comparing the three devices, the ideality factor for 1 μm and 2 μm are quite near to unity, indicating the better quality of the Schottky's contact under investigation and the absence of a thick interfacial layer [7].

Table 2: The data extracted from the I-V characteristics graph under the dark situation with different thicknesses of ZnO

| Doping Concentration ZnO (cm^{-3}) | Schottky Barrier Height (eV) | Ideality Factor (n) | Id at 5 V (A) | Ip at 5 V (A) | Rs (TW) |
|---|------------------------------|---------------------|---------------|---------------|----------|
| 0.5 | 0.6303 | 8.0612 | 3.93E-14 | 1.85E-06 | 127.2265 |
| 1 | 0.6939 | 1.5703 | 1.08E-12 | 8.17E-06 | 4.6296 |
| 2 | 0.7262 | 1.5336 | 1.43E-12 | 6.50E-06 | 3.4965 |

3.3. Spectral Response of ZnO/Si with Different Thickness of ZnO

The spectral response of ZnO/Si with three different thicknesses of ZnO is shown in Figure 6. Generally, the three devices exhibited photo response in the visible spectrum region, which is above 0.4 μm . For 0.5 μm of ZnO thickness, the peak current occurred at 0.5 μm ($E_G = 2.48$ eV), while for 1 μm and 2 μm devices, the peak current is at 0.6 μm ($E_G = 2.067$ eV). The spectra response indicated that the three devices had the potential for photodetection at the visible spectrum. It is interesting to note that the 1 μm device exhibited the highest photo response. Therefore, based on the I-V characteristics, the examination of the Schottky contact and the spectra response for the three different ZnO/Si devices, it can be said that 1 μm of ZnO thickness gives the optimum photocurrent responses with higher current gain, lower ideality factor, lower resistance, and highest photo response at the visible region.

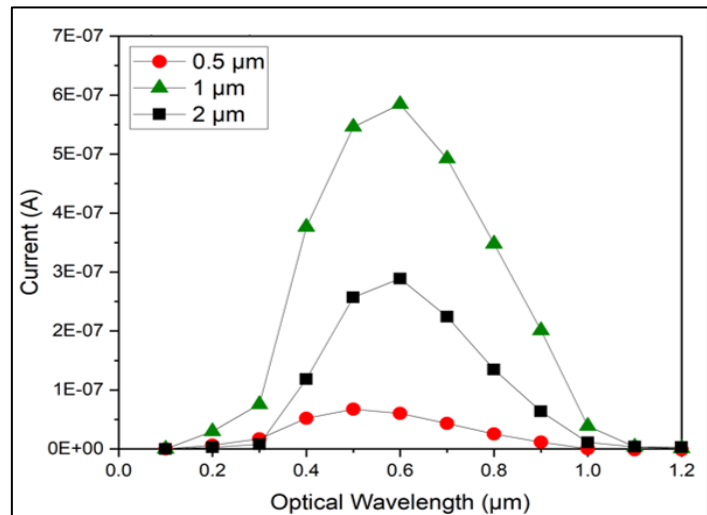


Figure 6: Spectral response of ZnO/Si with different thicknesses of ZnO

3.4. Structure and Net Doping of ZnO/Si with Three Doping Concentrations

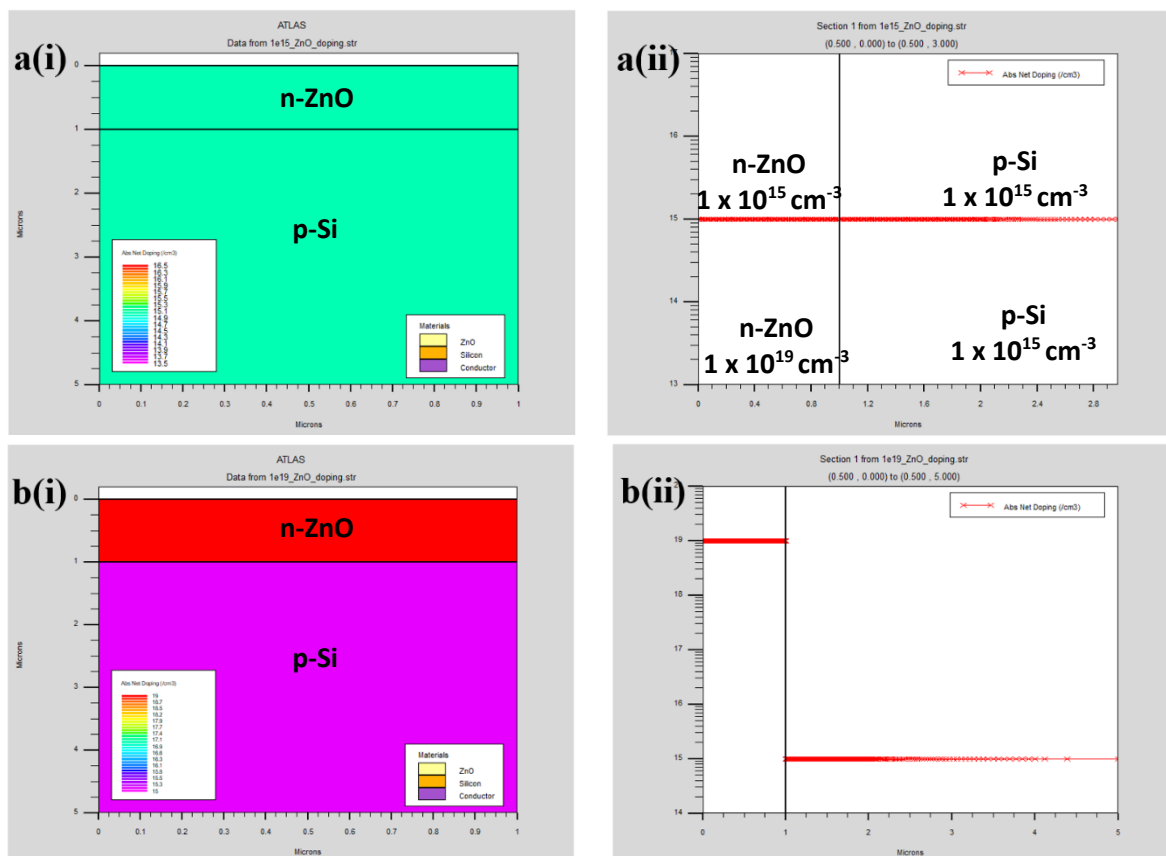


Figure 7: Structure and net doping of ZnO/Si with different doping concentration of a (i, ii) the substrate and ZnO doping= $1 \times 10^{15} \text{ cm}^{-3}$, b (i, ii) ZnO doping = $1, \times 10^{19} \text{ cm}^{-3}$

Figure 7 shows the structures that had been constructed and their net doping at the substrate and the ZnO layers for two conditions which are at ZnO doping of $1 \times 10^{15} \text{ cm}^{-3}$ and $1 \times 10^{19} \text{ cm}^{-3}$, respectively. Four different doping concentrations of ($1 \times 10^{15} \text{ cm}^{-3}$, $1 \times 10^{19} \text{ cm}^{-3}$, $1 \times 10^{20} \text{ cm}^{-3}$, $1 \times 10^{21} \text{ cm}^{-3}$) are being investigated in the study at the ZnO layer, while the doping concentration for the Silicon substrate is established at $1 \times 10^{15} \text{ cm}^{-3}$.

3.5. I-V Characteristics of ZnO/Si with Different Doping Concentrations of ZnO

Figure 8 shows the current-voltage characteristics of the ZnO/Si with different doping concentrations. It is observed that the dark currents for all the devices are shallow compared to the current under illumination, indicating the presence of the devices' photo response. These studies show that as ZnO increases from $1 \times 10^{15} \text{ cm}^{-3}$ to $1 \times 10^{21} \text{ cm}^{-3}$, the current under illumination also increases with the bias voltage. The highest photocurrent response is obtained from the $1 \times 10^{21} \text{ cm}^{-3}$ doping device, followed by the $1 \times 10^{20} \text{ cm}^{-3}$, $1 \times 10^{19} \text{ cm}^{-3}$ and $1 \times 10^{15} \text{ cm}^{-3}$ devices, respectively. A. Ali et al. showed that there was a limitation in the doping concentration of Zinc Oxide that will exhibit the maximum performance of the device. It is stated that the optimum doping concentration of Zinc Oxide is at 10^{19} cm^{-3} , and the efficiency of ZnO/Si drops immediately [14].

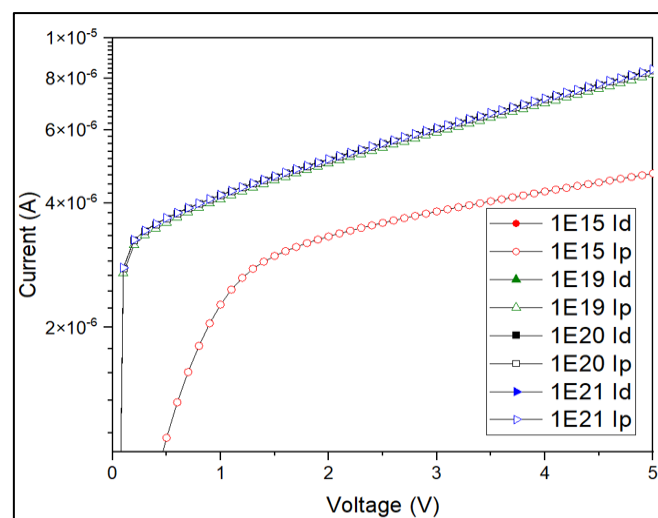


Figure 8: Current-voltage characteristics of ZnO/Si with a different doping concentration of ZnO

The performance evaluation for the photodetector can be probed by measuring the current gain. The gain of the ZnO/Si with different doping concentrations as a function of the bias voltage is shown in Figure 9. It is shown that the $1 \times 10^{15} \text{ cm}^{-3}$ doping concentration device obtains the highest current gain. It can be observed that as the doping concentration increases, the current gain decreases.

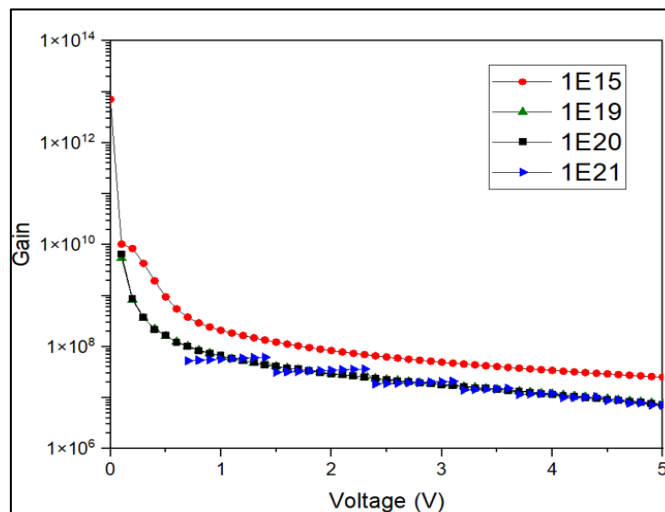


Figure 9: Gain of ZnO/Si with different doping concentrations of ZnO

The Schottky Barrier Height (SBH) is one of the crucial parameters to be calculated to examine the performance of the photodetector devices since the SBH is an energy level difference between the conduction or valence band toward the Fermi level for major carriers over a semiconductor metal interface. The barrier obstructs the flow of current from the metal to the semiconductor and thus controls the photodetectors' electronic transport [11]. The SBH and ideality factor for the ZnO/Si devices with different doping concentrations were extracted using the same method when extracting the data of SBH and ideality factor of ZnO/Si with different thicknesses in section 3.2.

Table 3 shows the data of SBH and ideality factor of the ZnO/Si with different doping concentrations of the ZnO layers. In general, it is shown that the SBH decreases when the doping concentration increases up to $1 \times 10^{20} \text{ cm}^{-3}$, but at $1 \times 10^{21} \text{ cm}^{-3}$ doping concentration, the value of SBH increases. Comparing the four devices, at $1 \times 10^{19} \text{ cm}^{-3}$ of doping concentration, it has the best ideality factor, which is at 1.5703 compared to $1 \times 10^{15} \text{ cm}^{-3}$ doping with the ideality factor at 4.3552, $1 \times 10^{20} \text{ cm}^{-3}$ doping at 2.5218 and $1 \times 10^{21} \text{ cm}^{-3}$ doping at 5.5529 respectively. The ideality factor of the $1 \times 10^{19} \text{ cm}^{-3}$ doping device is near unity compared to the other doping devices. A higher ideality factor of more than 2 implies that the diode exhibits non-ideal behavior due to the surface states and the oxide layer [15].

Table 3: The data extracted from the I-V characteristics graph under the dark situation with different doping concentrations of ZnO

| Doping Concentration ZnO (cm^{-3}) | Schottky Barrier Height (eV) | Ideality Factor (n) | Id at 5 V (A) | Ip at 5 V (A) | Rs (TW) |
|---|------------------------------|---------------------|---------------|---------------|---------|
| 1E15 | 0.7275 | 4.3552 | 1.86E-13 | 4.71E-06 | 26.8817 |
| 1E19 | 0.6939 | 1.5703 | 1.08E-12 | 8.17E-06 | 4.6296 |
| 1E20 | 0.6611 | 2.5218 | 1.16E-12 | 8.38E-06 | 4.3103 |
| 1E21 | 0.7457 | 5.5529 | 1.18E-12 | 8.41E-06 | 4.2373 |

3.6. I-V Spectral Response of ZnO/Si with Different Doping Concentrations of ZnO

Figure 10 shows the spectral response of the ZnO/Si with different doping concentrations of the ZnO layers. All the devices exhibited the peak photo response at same wavelength of 0.6 μm , which is in the visible spectrum. The $1 \times 10^{21} \text{ cm}^{-3}$ doping depicted the highest current response towards the light at 0.6 μm wavelength, followed by the 1×10^{20} and $1 \times 10^{19} \text{ cm}^{-3}$ doping devices respectively. The lowest current response towards light is by the 1×10^{15} doping concentration of ZnO. It is proven that all the doping concentrations of ZnO studied exhibited potential UV to visible photodetector since the spectral response is beyond the UV spectrum, which is between 0.4 and 1 μm .

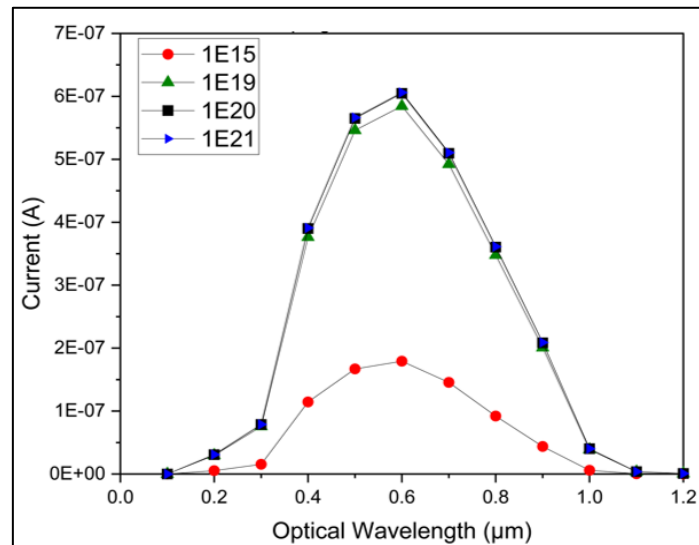


Figure 10: Spectral response of ZnO/Si with different doping concentrations of ZnO

4. CONCLUSION

In conclusion, the ZnO/Si with different thicknesses and doping concentrations of ZnO have been studied using SILVACO ATLAS tools. The performance of the ZnO/Si as UV to the visible photodetector device was brought to light. It can be concluded that the optimum thickness of ZnO is 1 μm on the 1 μm x 4 μm of the Silicon substrate. The Different thickness devices exhibited the photo current photo response from UV to the visible region with peaks occurring at 0.5 (m and 0.6 (m wavelength, respectively. The 1 μm thickness of the ZnO/Si device had the highest photo current response at 5 V bias (8.17 μA), and it also exhibited the highest peak current response towards the light at the 0.6 μm region in the spectral response.

The ZnO on Si devices has shown the potential for good UV to visible photodetector device since the light spectrum wavelength spans from 0.4 μm to about 1 μm . Meanwhile, the best doping concentration of the ZnO is at $1 \times 10^{21} \text{ cm}^{-3}$ since it exhibited the highest photocurrent response of 8.41 μA compared to the other devices. Meanwhile, for the spectral response, the $1 \times 10^{21} \text{ cm}^{-3}$ doping devices exhibited the highest current $1 \times 10^{21} \text{ cm}^{-3}$ doping devices exhibited the highest current response for spectral response at 0.6 μm .

ACKNOWLEDGEMENT

The author wishes to thank members of Universiti Teknologi MARA, Pulau Pinang Branch, USM, and Department of Applied Sciences, Universiti Teknologi MARA, Pulau Pinang Branch, for the unwavering technical assistance. The financial support from the Universiti Teknologi MARA through MyRA Research Grant Scheme (600-RMC/GPM ST 5/3 (042/2021) and Universiti Teknologi MARA, Cawangan Pulau Pinang is gratefully acknowledged.

CONFLICT OF INTEREST

The authors declare that there is no conflict of interest regarding the publication of this paper.

REFERENCES

- [1] Y. Zou, Y. Zhang, Y. Hu, and H. Gu, "Ultraviolet Detectors Based on Wide Bandgap Semiconductor Nanowire: A Review," *Sensors*, vol. 18, no. 7, p. 2072, 2018.
- [2] M. Razeghi and A. Rogalski, "Semiconductor ultraviolet detectors," *Journal of Applied Physics*, vol. 79, no. 10, pp. 7433-7473, 1996.
- [3] Y. Zhang, M. K. Ram, E. K. Stefanakos, and D. Y. Goswami, "Synthesis, Characterization, and Applications of ZnO Nanowires," *Journal of Nanomaterials*, vol. 2012, p. 624520, 2012.
- [4] A. Janotti and C. G. Van de Walle, "Fundamentals of zinc oxide as a semiconductor," *Reports on Progress in Physics*, vol. 72, no. 12, p. 126501, 2009/10/22 2009.
- [5] S. Sharma, A. Sumathi, and C. Periasamy, "Photodetection Properties of ZnO/Si Heterojunction Diode: A Simulation Study," *IETE Technical Review*, vol. 34, no. 1, pp. 83-90, 2017.
- [6] S. Sharma and C. Periasamy, "Simulation Study and Performance Analysis of n-ZnO/p-Si Heterojunction Photodetector," *Journal of Electron Devices*, vol. 19, pp. 1633-1636, 2014.
- [7] A. Abd Rahim *et al.*, "Investigation of light trapping mechanism of Silicon solar cell performance utilizing Silvaco TCAD," in *Journal of Physics: Conference Series*, vol. 1535, no. 1: IOP Publishing, p. 012021, 2020.
- [8] M. Manoua *et al.*, "Optimization of ZnO thickness for high efficiency of n-ZnO/p-Si heterojunction solar cells by 2D numerical simulation," in *2020 IEEE 6th International Conference on Optimization and Applications (ICOA)*, 20-21 April 2020, pp. 1-5, 2020.
- [9] L. Chabane, N. Zebbar, M. Trari, and M. Kechouane, "Opto-capacitive study of n-ZnO/p-Si heterojunctions elaborated by reactive sputtering method: Solar cell applications," *Thin Solid Films*, vol. 636, pp. 419-424, 2017.
- [10] A. Rouis, N. Hizem, and A. Kalboussi, "Electrical characterizations of Schottky diode with zinc oxide nanowires," in *2019 IEEE International Conference on Design & Test of Integrated Micro & Nano-Systems (DTS)*, 28 April-1 May 2019, pp. 1-5, 2019.
- [11] A. F. Abd Rahim, M. R. Hashim, and N. K. Ali, "High sensitivity of palladium on porous silicon MSM photodetector," *Physica B: Condensed Matter*, vol. 406, no. 4, pp. 1034-1037, 2011.
- [12] M. Asghar, K. Mahmood, M. Faisal, and M. A. Hasan, "Electrical characterization of Au/ZnO/Si Schottky contact," *Journal of Physics: Conference Series*, vol. 439, p. 012030, 2013.
- [13] T. Varma, C. Periasamy, and D. Boolchandani, "Performance analyses of Schottky diodes with Au/Pd contacts on n-ZnO thin films as UV detectors," *Superlattices and Microstructures*, vol. 112, pp. 151-163, 2017.
- [14] A. Ali, B. Hussain, and A. Ebong, "Computer modeling of n-ZnO/p-Si single heterojunction bifacial solar Cell," in *2016 IEEE 43rd Photovoltaic Specialists Conference (PVSC)*, 5-10 June 2016 2016, pp. 0591-0594, 2016.

- [15] F. Z. Bedia, A. Bedia, B. Benyoucef, and S. Hamzaoui, "Electrical Characterization of n-ZnO/p-Si Heterojunction Prepared by Spray Pyrolysis Technique," *Physics Procedia*, vol. 55, pp. 61-67, 2014.